



Spectroscopically Identified Cataclysmic Variables from the LAMOST Survey. I. The Sample

Wen Hou¹, A-li Luo^{1,2,3,4} , Yin-Bi Li¹, and Li Qin^{1,2,3}

¹ Key Laboratory of Optical Astronomy, National Astronomical Observatories, Chinese Academy of Sciences, 20A Datun Road, Chaoyang District, Beijing, 100101, People's Republic of China; lal@nao.cas.cn, whou@nao.cas.cn

² University of Chinese Academy of Sciences, Beijing 100049, People's Republic of China

³ School of Information Management & Institute for Astronomical Science, Dezhou University, Dezhou 253023, People's Republic of China

⁴ Department of Physics and Astronomy, University of Delaware, Newark, DE 19716, USA

Received 2019 June 27; revised 2019 November 14; accepted 2019 November 17; published 2020 January 10

Abstract

A sample of cataclysmic variables (CVs) is presented including spectroscopically identified 380 spectra of 245 objects, of which 58 CV candidates are new discoveries. The BaggingTopPush and the Random Forest algorithms are applied to the Fifth Data Release (DR5) of the Large Sky Area Multi-Object Fiber Spectroscopic Telescope (LAMOST) to retrieve CVs with strong emission lines and with broad absorption lines respectively. Based on spectroscopic classification, 134 dwarf novae, 41 nova-like variables, and 19 magnetic CVs are identified from the sample. In addition, 89 high-inclination systems and 33 CVs showing companion stars are recognized and discussed for their distinct spectral characteristics. Comparisons between CVs from LAMOST and from published catalogs are made in spatial and magnitude distribution, and the difference of their locus in the *Gaia* color–absolute magnitude diagram (CaMD) are also investigated. More interestingly, for two dwarf novae observed through LAMOST and SDSS in different epochs, their spectra both in quiescence phase and during outburst are exhibited.

Unified Astronomy Thesaurus concepts: Cataclysmic variable stars (203); Dwarf novae (418); Nova-like variable stars (1126); Catalogs (205); Astronomy data analysis (1858)

Supporting material: machine-readable table

1. Introduction

Cataclysmic variables (CVs) are semi-detached binaries with very short orbital periods, in which white dwarf primaries accrete matter from low-mass secondaries. The secondaries are usually late main-sequence stars, and in a few cases, they may also be highly evolved stars such as AM CVn type stars. CVs have been classified according to their amplitudes and time-scale of variability, which are classical novae (CN), recurrent novae (RN), dwarf novae (DN), and nova-like variables (NL). Besides the above classification, there is also an important group called magnetic CVs which consist of polars and intermediate polars. Regarding the main characteristics of these objects, a more detailed description can be found in Warner (2003) and Kogure & Leung (2007).

Up to now, several catalogs of CVs have been published. An early catalog and atlas of CVs was provided by Downes et al. (2001) combining and supplementing the first two editions (Downes & Shara 1993; Downes et al. 1997), which finally consists of 1034 CVs containing the basic information of parameters such as coordinates, subtypes magnitudes, orbital periods, etc. Among these CVs, over 60% of the objects have available spectra, including 49% spectra in quiescence and 15% spectra during outburst. One of the most comprehensive investigations of CV spectra from the large-scale sky surveys was performed by Szkody et al. (2002). A series of papers (Papers I–VIII) have been published between 2002 and 2011 to explore the properties of the 285 CVs identified from the Sloan Digital Sky Survey (SDSS) I/II (Szkody et al. 2002, 2003, 2004, 2005, 2006, 2007, 2009, 2011). Owing to the capability of SDSS to observe faint CVs, Szkody et al. (2011) analyzed the distribution of orbital periods of CVs from SDSS, which is quite different from previous results. Also dedicated to the

study of orbital periods of faint CVs from SDSS, Gänsicke et al. (2009) discussed the period distribution of a sample which contains a large fraction of short-period CVs. Besides, with the operation of the Catalina Real-time Transient Survey (CRTS), plenty of studies have sprung up to investigate the properties of CVs. Drake et al. (2014) provided a sample of 855 CV candidates observed by CRTS, of which 205 targets were discovered for the first time and 137 targets were identified through spectra. Woudt et al. (2013) presented high-speed photometric observations of dozens of faint CVs selected from SDSS and CRTS. Likewise for faint CVs, Breedt et al. (2014) examined spectroscopic properties of 85 CVs using both SDSS and follow-up spectroscopic observations, and analyzed the photometric properties of 1043 CV systems from CRTS. Moreover, Mróz et al. (2015) gave the largest sample of 1091 DN (one subclass of CV) located in the Galactic bulge from the Optical Gravitational Lensing Experiment (OGLE) survey. Thus far, large-scale sky surveys, either spectroscopic or photometric, show great potential to search for candidates of CVs.

The Large Sky Area Multi-Object Fiber Spectroscopic Telescope (LAMOST) took its first light in 2008 (Cui et al. 2012). After two years of commissioning and one year of pilot survey, LAMOST started a five-year regular survey. The survey mainly focused on the Milky Way and archived several millions of stellar spectra in the Fifth Data Release (DR5). This massive database is a rich source for detecting CVs, which arouses great interest of researchers being devoted to the studies of CVs. Jiang et al. (2013) proposed a data-mining method by combining the support-vector machine (SVM) with the principal component analysis (PCA) to search for CVs with the commissioning data of LAMOST. They identified a sample of 10 CVs, two of which are new discoveries. Han et al. (2018) collected the spectra of 48

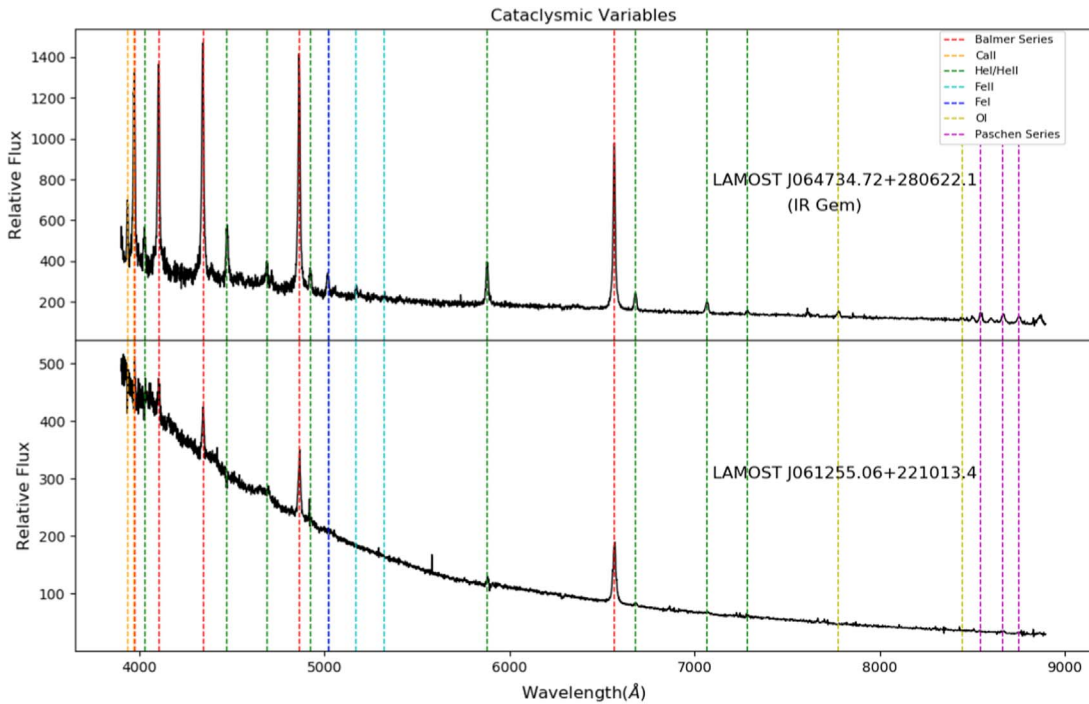


Figure 1. Two examples of CV spectra with significant emission lines from the LAMOST survey. Some strong emission lines are marked in different colors in the spectra. We also show the LAMOST designations of objects in the figure.

known CVs by cross-matching the published catalogs with LAMOST DR3, and found three new CVs using the method proposed by Jiang et al. (2013). They investigated not only spectroscopic properties of all these CVs, but also light curves of five CVs through follow-up photometric observations. Common to these CV search efforts is the use of strong emission lines in spectra or some of the properties of known CVs recorded in the literature. So far, there has not been a systematic and comprehensive investigation on CVs using LAMOST data. In this paper, we focus on the search of CVs in different subtypes as well as the analysis of spectral features of each subtype. Further study on orbital periods has begun and the results will be included in a later paper.

We conduct a comprehensive search of CVs in LAMOST DR5 using machine learning methods. According to different spectroscopic characteristics of CV subtypes, we categorize as many CVs found in LAMOST DR5 as possible. The paper is organized as follows. The observation and the data in LAMOST DR5 are briefly introduced, and the selection process for the initial sample among which we search for CV candidates is presented in Section 2. The methods adopted to search for two groups of CVs with different spectral characteristics are given in detail in Section 3. Then the sample of CVs from LAMOST DR5 is studied in Section 4, including features and classification of CV subtypes, the distributions in space, in magnitude, and in the *Gaia* color–absolute magnitude diagram (CaMD), as well as spectra of common targets both in LAMOST and SDSS data sets. An analysis of 58 new discoveries and a description of the CV catalog are also included in Section 4. Finally, some discussions and summaries for the work are given in Section 5.

2. Observations and Data Reduction

Undertaken by the Chinese Academy of Science, the LAMOST survey has become the first spectroscopic survey to collect tens of

millions spectra from the universe. Owing to the unique design of LAMOST, it is able to acquire 4000 spectra simultaneously in a single exposure with a limiting magnitude as faint as $r \sim 18$ at the resolution of 1800. The wavelength range for these low resolution spectra covers the optical band from 3700 to 9000 Å. The LAMOST survey contains two major components including the LAMOST ExtraGalactic Survey (LEGAS) and the LAMOST Experiment for Galactic Understanding and Exploration (LEGUE) survey (Deng et al. 2012; Zhao et al. 2012). The raw data has been processed by LAMOST pipelines to extract, calibrate, as well as classify the spectra, which were described in detail in Luo et al. (2012, 2015). With the released spectra, objects have been classified as galaxies, quasi-stellar objects (QSOs), and stars, and stars have been further classified into seven subtypes along the temperature sequence as well as into special types such as white dwarfs, double stars, carbon stars, etc.

So far, the LAMOST survey has been conducted for about 8 yr since 2011, including a one-year pilot survey followed by an ongoing regular survey. The LAMOST-I regular survey was defined as from 2012 September to 2017 June, which covers approximately 17,000 square degrees of the sky. The data of LAMOST-I survey together with the pilot survey make up the DR5, which has been available to the public since 2019 June (A.-L. Luo et al. 2019, in preparation). The total number of spectra in DR5 is more than 9 million, including 152,863 galaxies, 52,453 QSOs, 8,183,160 stars, and 637,889 objects with unclassified type. Among the massive data, there are about 6 million spectra of which the signal-to-noise ratios (S/N) per pixel for both the *g* band and the *i* band are larger than 10. Along with the general catalog, another three specific samples selected from the whole sample were also released as separate catalogs, including a catalog of 5,348,712 late-A, -F, -G, and -K stars with atmospheric parameters (i.e., T_{eff} , $\log g$, and $[\text{Fe}/\text{H}]$), a catalog of $\sim 439,920$ A-type stars, and a catalog of $\sim 534,393$ M dwarfs.

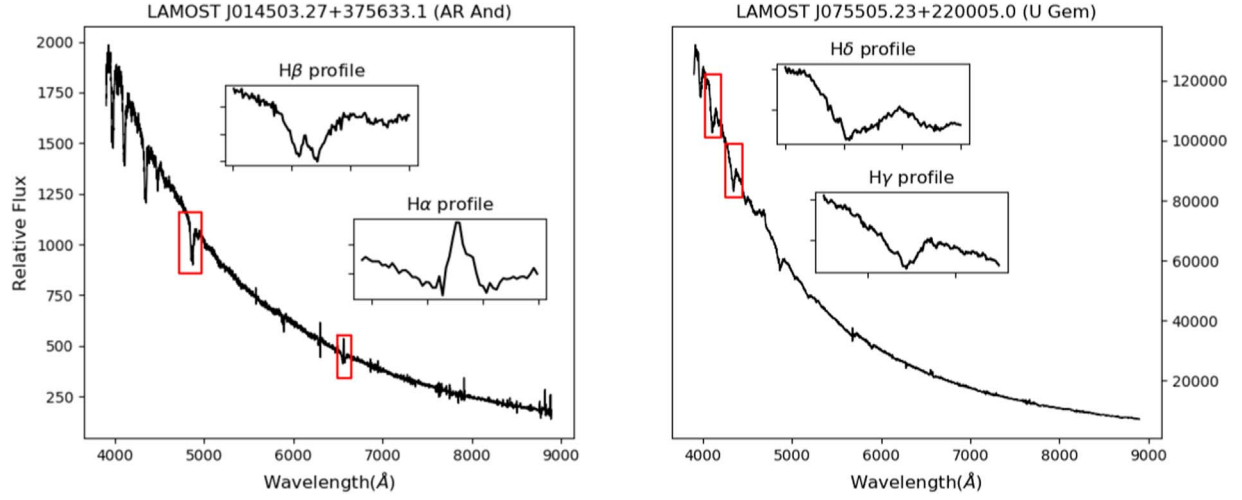


Figure 2. Two spectra of CVs with broad absorption lines from the LAMOST survey, which show identical spectral characteristics. The profiles of $H\alpha$ and $H\beta$ of the left spectra and $H\gamma$ and $H\delta$ of the right spectra are plotted in the figure. Emission components appear in both the $H\alpha$ and $H\beta$ lines, but are absent in $H\gamma$ and $H\delta$.

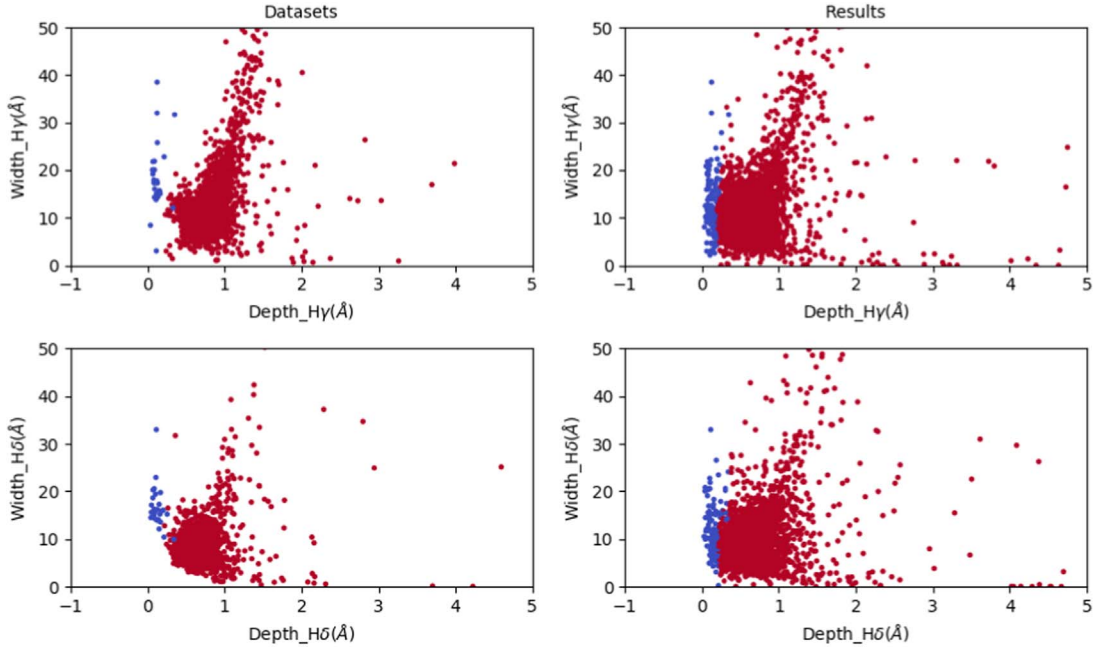


Figure 3. Result of CV candidates using the Random Forest algorithm based on $H\gamma$ and $H\delta$ line features. The positive and negative data sets are shown in the two left panels and the result using the Random Forest method are shown in the right panels. The CV spectra are represented by blue points and O/B/A-type spectra are plotted as red points.

In this work, we carry out a comprehensive search of CVs in LAMOST DR5, in which we first need to define a search range in the whole released data set. Considering the spectral characteristics, a large portion of CVs were probably misclassified as O/B/A stars or white dwarfs by the LAMOST pipeline because of the template matching algorithm it used. Even for those having been classified as CVs by the pipeline, we find that over 97% of them are actually spectra of normal stars that are contaminated by superimposing some nebular emission lines from H II regions, and only $\sim 3\%$ are spectra of real CVs. To collect as much CV spectra as possible, the “unknown” objects in DR5 should also be taken into account since the pipeline refuses to classify some “bad” spectra, which results in a few CVs hidden in the unknown data set. To sum up, we select a total of $\sim 1130,000$ spectra to be the initial

sample we begin with the search, including $\sim 480,000$ O/B/A stars, $\sim 20,000$ white dwarfs, ~ 3000 CVs, and $\sim 630,000$ unknown spectra.

3. Methods

According to the spectral characteristics, we search for two types of CV spectra that display significantly different features. One type of CV spectra are dominated by obvious emission lines, which are probably DN in quiescence or NL variables. The other type of CV spectra show broad absorption lines where emission lines are overwhelmed by their continuum, which are probably CVs in outburst status or CVs surrounded by optically thick disks. We need to adopt different methods to select the candidates of these two groups, respectively.

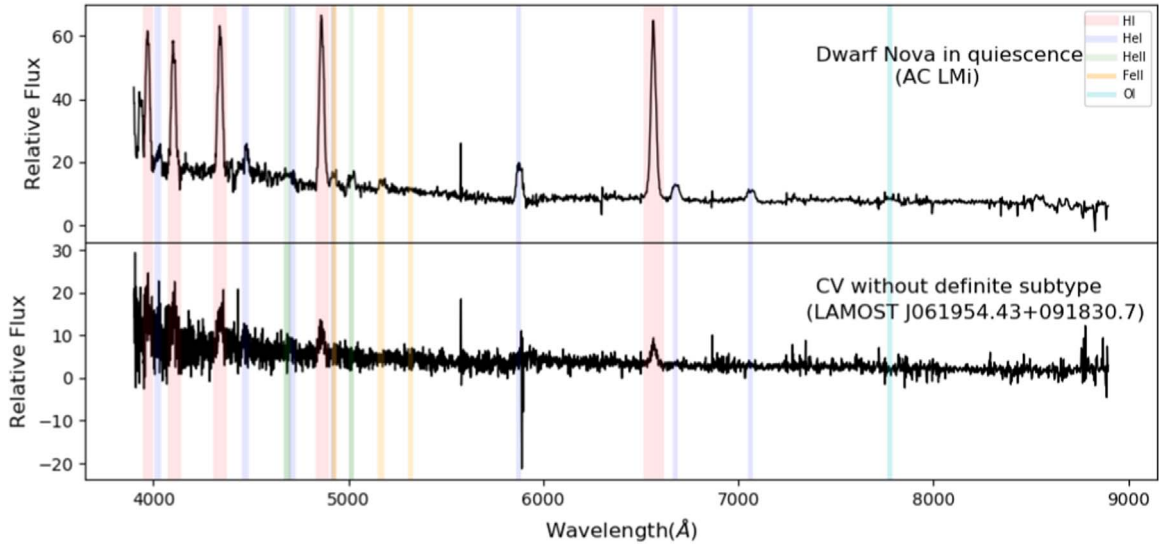


Figure 4. Spectra of DN in quiescence and CV without a definite subtype from LAMOST DR5. The common spectral lines shown in the DN spectrum are marked by different colors for different elements, including H I, He I, He II, Fe II, and O I. A spectrum of CV without a definite subtype is plotted in the bottom panel. Due to its low S/N, the spectral features cannot be seen clearly except for the strong Balmer emission lines.

Table 1
Basic Emission-line List for Spectra of Quiescent DN in the Optical Region

| Wavelength (Å) | Spectral Line | Wavelength (Å) | Spectral Line | Wavelength (Å) | Spectral Line |
|----------------|---------------|----------------|---------------|----------------|------------------|
| 3934 | Ca II | 4861 | H β | 8438 | P18 |
| 3968 | Ca II | 4922 | He I | 8446 | O I |
| 3970 | He I | 4924 | Fe II | 8467 | P17 |
| 4026 | He I | 5016 | He II | 8498 | Ca II |
| 4102 | H δ | 5018 | Fe I | 8502 | P16 |
| 4121 | He I | 5169 | Fe II | 8542 | Ca II |
| 4634–42 | N III | 5317 | Fe II | 8545 | P15 |
| 4340 | H γ | 5876 | He II | 8598 | P14 |
| 4388 | He I | 6563 | H α | 8662 | Ca II |
| 4471 | He I | 6678 | He I | 8665 | P13 |
| 4634–42 | C III | 7065 | He I | 8750 | P12 |
| 4647–51 | N III | 7281 | He I | 8863 | P11 |
| 4686 | He II | 7772,74,75 | O I | 9015 | P10 |
| 4713 | He I | 8236 | He II | 9229 | P9(+Fe II,Mg II) |

For the two groups with specific features of CVs, some known CV spectra are needed as templates to pick up the candidates in the initial data set. We first collect the CV catalogs from the literatures as well as the SIMBAD database, which eventually contain 4215 CVs without being removed duplicate sources (Downes & Shara 1993; Wenger et al. 2000; Downes et al. 2001; Szkody et al. 2011; Breed et al. 2014; Coppejans et al. 2014, 2016; Drake et al. 2014). Cross-matching known CVs and LAMOST catalogs within a cross radius of $5''$, about 500 LAMOST spectra of known CVs are obtained. After visually checking these spectra, more than half of the spectra are difficult to be recognized as CVs due to their low S/N (<3). Besides, There is also a small number of spectra showing general characteristics of F-, G-, or K-type spectra without any emission lines, which are likely not CVs. Finally, 155 spectra are identified to display the detectable characteristics of CVs. Among the 155 CV spectra, we select 75 high-quality spectra as templates to search for two groups of CVs separately, in which 50 spectra are in one group having strong emission lines and 25 spectra are in another group with broad absorption lines.

3.1. Spectra Dominated by Emission Lines

The CV spectra of this group are characterized by their significant emission lines, such as Balmer series and/or He I/He II. Such obvious features could be easily hunted in a big data set using a so-called BaggingTopPush algorithm developed by Du et al. (2016), which combines a bipartite ranking model with the bootstrap aggregating techniques. The core idea of the BaggingTopPush approach is to build a ranking model that ranks the unlabelled samples based on their relevance scores to the positive samples (the given templates). The method was effectively applied to search for carbon stars from SDSS DR10 and LAMOST DR4 performed by Du et al. (2016) and Li et al. (2018). A detailed introduction and application of this method can be referred to in Du et al. (2016). The reason why we adopt this method is considering its advantage that the expert knowledge can be taken into account when checking the ranked result.

In the training stage, 50 CV templates collected from the known CV catalogs mentioned above are considered as the positive samples. Figure 1 shows two examples of CV spectra as templates from LAMOST DR5. All the spectra of this type

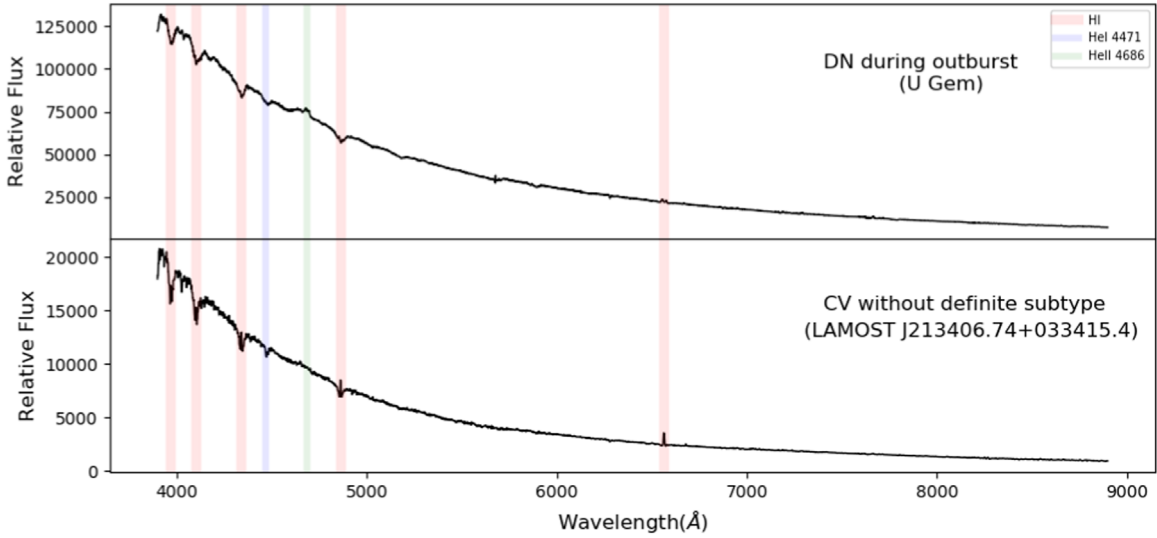


Figure 5. The spectra of DNs undergoing outburst and CV without a definite subtype from LAMOST DR5. The main absorption features and wide emission line He II $\lambda 4686$ shown in the DN during outburst are marked by different colors for different elements in the top panel. For the CV in the bottom panel, broad absorption lines such as Balmer series and He I $\lambda 4471$ are also shown in the spectrum. Besides, there are no obvious emission lines, apart from H α emission and narrow emission cores in higher order of Balmer line profiles.

Table 2

Additional Emission Lines in the Spectra NL Variables in the Optical Region

| Wavelength (Å) | Spectral Line | Wavelength (Å) | Spectral Line |
|----------------|---------------|----------------|---------------|
| 3819 | He I | 4267 | C II |
| 4070–76 | O II | 4415–17 | O II |
| 4089 | S II | 4542 | He II |
| 4128–30 | S II | 5805 | C IV |
| 4143 | He I | 7234 | C II |

display strong emissions of Balmer series including H α , H β , H γ , H δ , and H ϵ . Other emission lines such as He I, He II, and Fe II also frequently appear in these spectra, not as strong as Balmer emission lines. According to the spectral features, a CV spectrum dominated by strong emission lines is probably classified as either an O/B/A-type star, a white dwarf, a CV, or even an unknown object by the LAMOST pipeline. Thus we need to search for this kind of CV in the whole initial data set containing 1130,000 spectra, which is divided into 10 groups to apply the BaggingTopPush. Empirically, we manually check the result of top 1000 spectra for each of the 10 groups. We notice that the false CVs in the top thousand spectra are mainly spectra superimposed nebula emissions. In addition, the lower the ranking, the fewer CVs are found, and there are almost no CVs in the bottom 500 objects. We eventually obtain 256 spectra of CV candidates exhibiting strong emission lines.

3.2. Spectra with Broad Absorption Lines

Another group of CV spectra exhibit their main feature of broad absorption spectral lines along with weak emissions in the core (mostly in H α or H β). As mentioned above, these objects contain different types of CVs, such as DN in outburst and CVs with lower disk luminosity. An example of two spectra of this type from the LAMOST survey are shown in Figure 2, which shows the bright blue continua and broad absorption Balmer lines. It is likely that the LAMOST pipeline misclassified nearly all of this kind of CV as O/B/A stars or white dwarfs due to the high

similarity between O/B/A stars or white dwarfs with CVs in spectra. Therefore, we select this kind of CV spectra from O/B/A stars, white dwarfs, and CVs in DR5, which includes more than 470,000 spectra. In addition, since spectral features of this kind of CV are not as prominent as CV spectra with emission lines, we use both the BaggingTopPush approach and the method of Random Forest based on the width and depth of Balmer lines to select as many CV candidates of this type as possible.

3.2.1. Preliminary Selection

In the spectra of these CVs, low-order Balmer lines such as H α and H β always show emissions in the cores, and higher-order Balmer series show broad absorption lines. Therefore, we first pick up spectra with H α in the emission from more than 470,000 O/B/A, white dwarf, and CV spectra using the method proposed by Hou et al. (2016). The method aims to figure out two different profile shapes of strong H α emission lines as well as weak emission lines lying in the deep H α absorption profiles in the spectra. By applying the following criteria, we select about 17000 spectra with H α emission lines from $\sim 470,000$ spectra.

$$\sum_{i=-5}^5 f_{\text{obs}}[n_0 + i]/11 > f_{\text{conti}}[n_0] \quad (1)$$

$$\sum_{i=-1}^1 f[n_0 + i]/3 > \sum_{i=-2}^2 f[n_0 + i]/5 \text{ \& } \max(f_{\text{obs}}[n_0 - 1 : n_0 + 1]) \geq \max(f_{\text{obs}}[n_0 - 2 : n_0 + 2]), \quad (2)$$

where n_0 is the pixel index of central wavelength of H α ($\lambda_0 = 6564 \text{ \AA}$), f_{obs} , f_{conti} denote the flux for observed spectra and continuum spectra, respectively, and $\max(f_{\text{obs}}[x:y])$ represents the maximum flux where the index is from x to y .

3.2.2. The BaggingTopPush Approach

The same as the method used in Section 3.1, we also adopt the BaggingTopPush approach to select CVs with broad

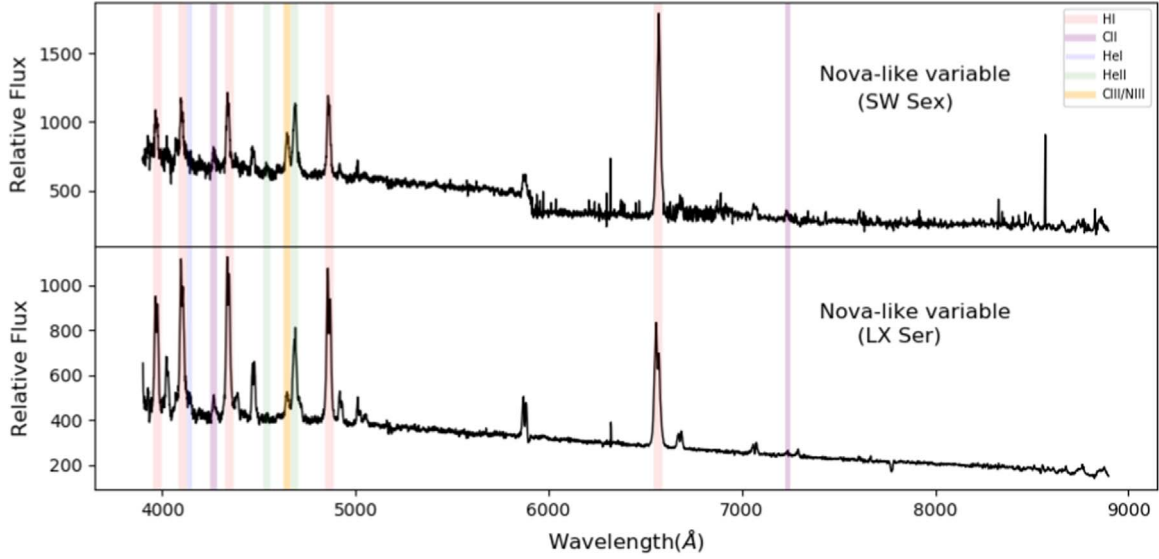


Figure 6. Spectra of NL from LAMOST DR5. Balmer series and the wide emission line He II $\lambda 4686$ and C III/N III $\lambda 4650$ blend are shown in the spectra. In addition, some unique spectral lines in the NL spectra including C II and He I are also shown. These emission lines are marked by different colors for different elements.

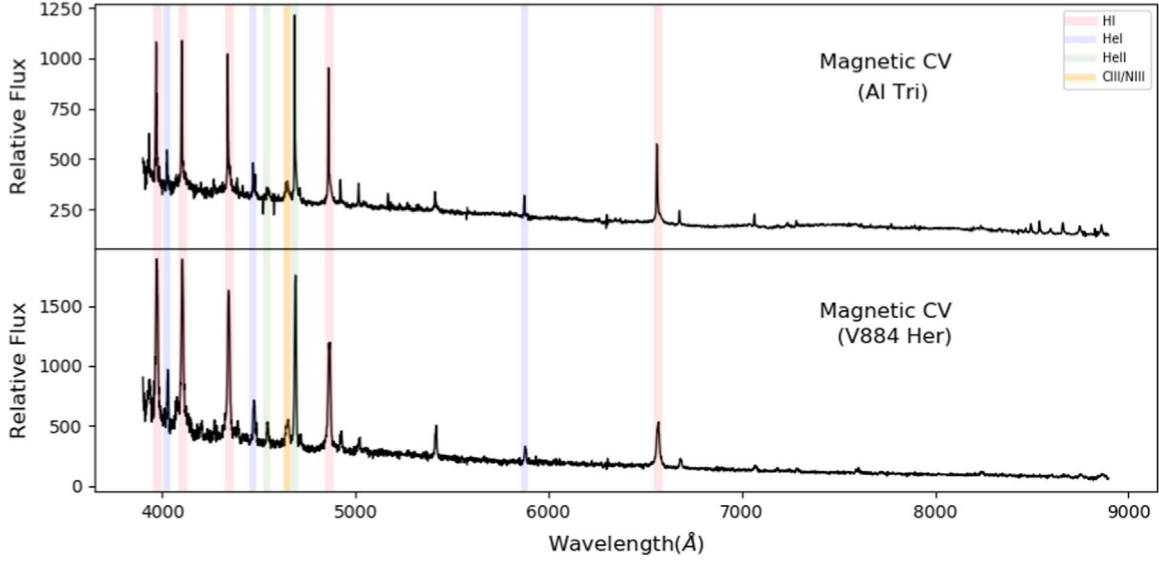


Figure 7. Spectra of magnetic CVs from LAMOST DR5. The significant spectral lines including Balmer series and the He II $\lambda 4686$ and C III/N III $\lambda 4650$ blend are shown in the spectra. These emission lines are marked by different colors for different elements.

absorption lines from about 17000 spectra showing $H\alpha$ emissions. 25 CV templates with broad absorption lines picked up from the known CVs are considered as the positive samples when we apply the method to 17000 spectra. Similarly, we checked the top 10,000 spectra by experience and finally pick up 91 CVs showing broad absorption lines. However, due to the less significant characteristics of this kind of CV spectra, it is not as effective as searching for CV spectra with strong emission lines as in Section 3.1. A more efficient classification method is adopted as an important supplement for picking up CV spectra with broad absorption lines, which is described in the following subsection.

3.2.3. Spectral-line-based Random Forest

Two obvious differences between the spectra of CVs with broad absorption lines and another type with $H\alpha$ emissions are the line widths and depths of the Balmer series. Different for

the 17000 spectra with $H\alpha$ emissions, the $H\alpha$ and $H\beta$ of these CV spectra often show emission cores, while the higher-order Balmer series such as $H\gamma$ and $H\delta$ basically have pure broad absorption lines. So we fit $H\gamma$ and $H\delta$ lines by a Gaussian function to obtain both the line widths and line depths, which can be used to distinguish CVs from other types stars. We then use the Random Forest algorithm to effectively select samples of CVs based on these line widths and depths.

The 25 absorption line CVs mentioned above are fed to the Random Forest algorithm as positive templates. For the negative data set, we randomly select 5000 spectra classified by the LAMOST pipeline as normal O/B/A-types. As shown in Figure 3, the two left panels show the distributions of line features of templates, in which the CV templates are plotted in blue and the O/B/A-type spectra are in red. The line features of $H\gamma$ and $H\delta$ of $\sim 170,000$ spectra from LAMOST DR5 are plotted by red points in the right panels, and the blue ones represent the

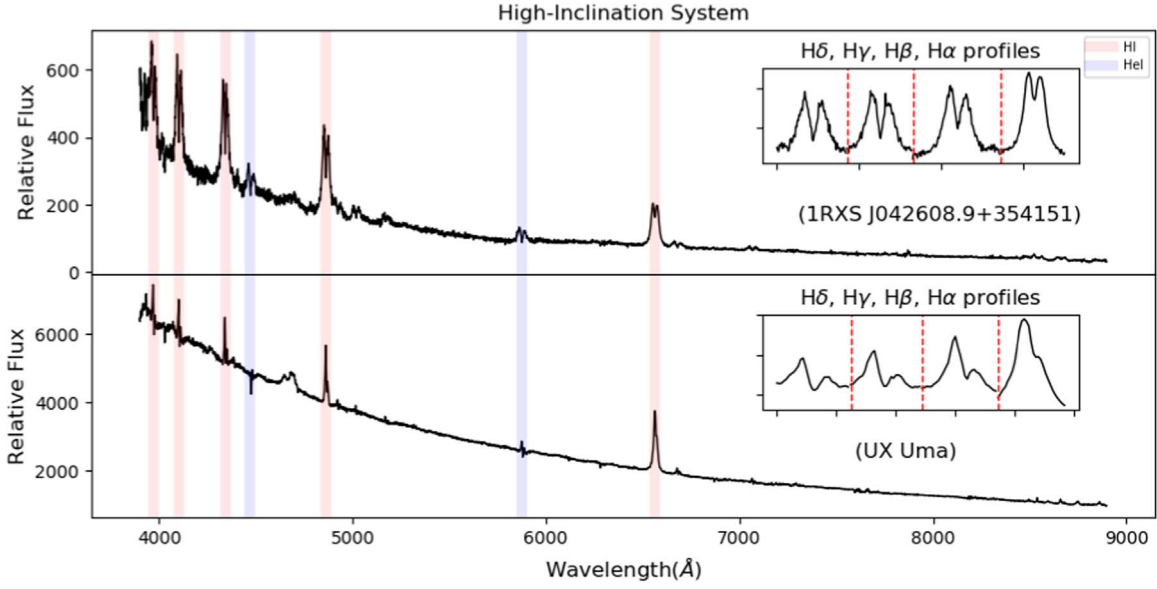


Figure 8. Spectra of high-inclination systems from LAMOST DR5. Spectral line profiles exhibiting a double peak can be seen clearly in the spectra, such as Balmer series and He I emission lines. Double-peak profiles are marked by different colors for different elements. Besides, close-ups of the $H\alpha$, $H\beta$, $H\gamma$, and $H\delta$ profiles for each spectrum are shown in the subgraph.

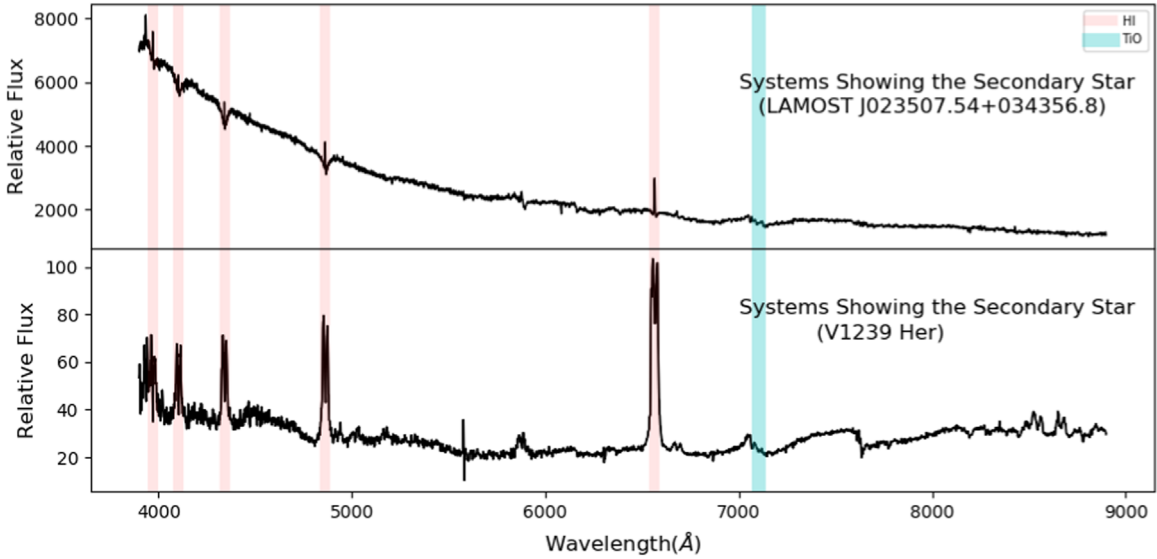


Figure 9. Spectra of CV systems showing secondary stars from LAMOST DR5. Both spectra exhibit characteristics of a M-type star at the 7100 Å band. For the top spectrum, the emission lines are quite narrow lying in the broad absorption lines. For the bottom spectrum, the emission lines show deep central absorption reverses, which is a typical feature of a high-inclination system.

CV candidates selected by the Random Forest algorithm using the line features of $H\gamma$ and $H\delta$. The final CV candidates are the intersection data set of the Random Forest results from the $H\gamma$ and $H\delta$ line features, and they are also checked by the careful manual inspection. In combination with the results of the BaggingTop-Push approach and the Random Forest method, we finally pick out 124 CV candidates with broad absorption lines.

4. Results

A total of 380 spectra of CVs, which correspond to 245 unique objects, are found in LAMOST DR5. By cross-matching with 4976 known CVs collected from previous literature, 58 out of 245 are newly discovered candidates that have no record in the published CV catalogs.

4.1. Spectral Features

For the 380 CV spectra, we calculate the equivalent widths of prominent Balmer lines, He I $\lambda 4471$ and He II $\lambda 4686$, as well as the ratio of $H\beta$ to He II $\lambda 4686$. For most CVs with strong emission lines, the Balmer decrement from $H\alpha$ to $H\delta$ becomes shallow or sometimes even negative, which is consistent with that of Warner (2003).

Although the classification of CVs is generally based on their amplitudes and timescale of the variabilities, we can still see some clues through spectral features. The main spectral characteristics to classify CV subtypes include He II emission lines, Fe II emission lines, high-excitation emission lines such as C III and N III, as well as the line ratio of $H\beta$ to He II $\lambda 4686$. In order to determine the subtype of CVs, we manually inspect

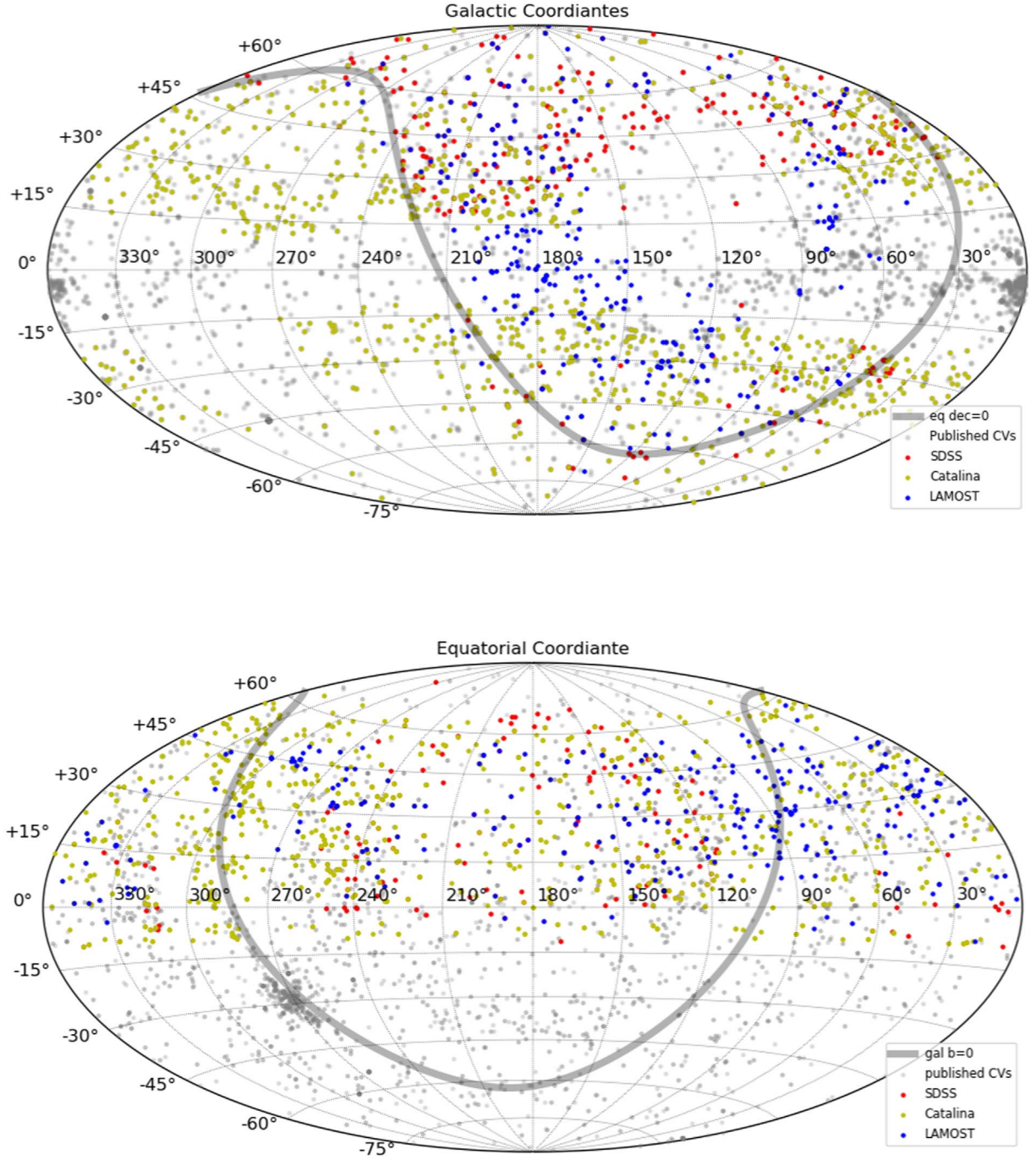


Figure 10. Spatial distributions of CVs from different catalogs in galactic and equatorial coordinates. For both coordinates systems, the gray points represent all CVs collected from the published catalogs. In particular, CVs from the SDSS and Catalina survey are plotted by red and yellow points, respectively. CVs selected from LAMOST DR5 are represented by the blue points. The spatial distributions of CVs from these three surveys are different from each other.

all the spectra, compare the intensities of $H\beta$ with $He\ II\ \lambda 4686$, and check the existence of unique spectral lines in each subtype of spectra. Based on the spectral features, we assign subtypes to as many of the CVs as possible. A detailed description of the classification follows.

Dwarf Nova (DN). Table 1 shows the basic emission lines appearing in the spectra of DN in quiescence. For spectra of quiescent DNs, prime characteristics include a large ratio of $H\beta$ to $He\ II\ \lambda 4686$ as well as a weak or absent blended $C\ III/N\ III\ \lambda 4650$ (Warner 2003). We check 95 quiescent spectra in our sample, which are classified as DN in previous literature. As a

result, the value of $H\beta/He\ II\ \lambda 4686$ are larger than 2 for almost all the spectra of DN in quiescence, except those spectra that have too low S/N to calculate the accurate line intensity. Another important characteristic is that Fe emission lines always appear in the spectra of DN, such as $Fe\ II\ \lambda 4924$, $\lambda 5169$, and $\lambda 5317$. According to the criteria mentioned above, CV spectra from LAMOST DR5, which have the value of $H\beta/He\ II\ \lambda 4686 > 2$ and display the emission line of iron such as $Fe\ II\ \lambda 5169$, are regarded as the spectra of quiescent DN shown in Figure 4. The significant spectral lines in spectra of quiescent DN are marked by different colors in Figure 4. The $Fe\ II$

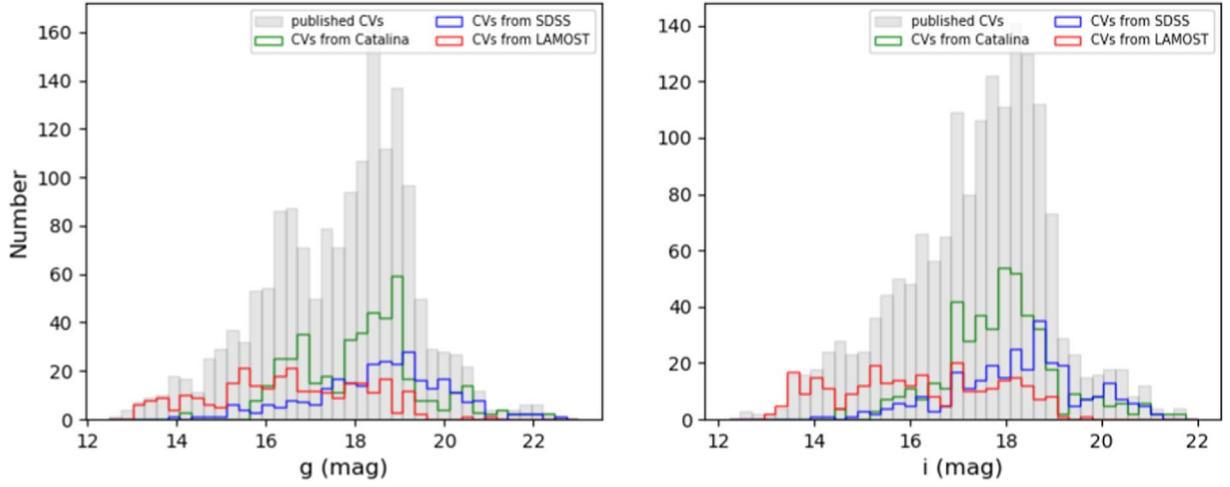


Figure 11. Magnitude distributions of g and i band for CVs from the published catalogs, Catalina, SDSS, and LAMOST surveys.

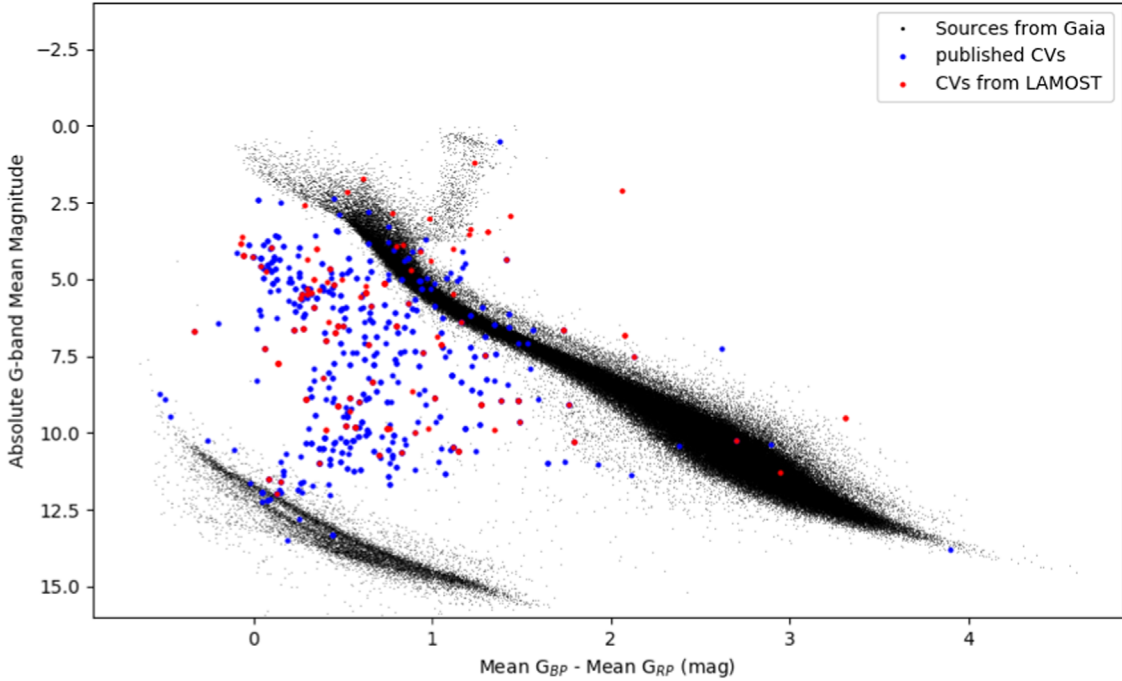


Figure 12. CVs from published catalogs and LAMOST in *Gaia* CaMD.

emission lines selected as one criterion of DN are marked by yellow in the figure, which include Fe II $\lambda 5169$, $\lambda 5317$, and Fe II $\lambda 4924$ blending with He I $\lambda 4922$. There is also a portion of CV spectra showing no obvious emission lines besides the Balmer series, like the spectrum in the bottom panel of Figure 4. Because most of the spectral characteristics are overwhelmed by noise, we are unable to make a definite subtype classification.

In addition, we also find several spectra of DN undergoing outburst. For these spectra, the distinct spectral characteristics include the absorption lines such as Balmer series and He I $\lambda 4471$, which have the similar widths to those of emission lines in quiescent spectra as well as a wide He II $\lambda 4686$ emission line. A spectrum of DN undergoing outburst is shown in the top panel of Figure 5, in which main broad absorption lines and the He II $\lambda 4686$ emission line are marked by different colors. Besides, some other spectra also show similar absorption

features to those of DN undergoing outburst, as seen in the bottom panel of Figure 5. In these spectra, narrow emission cores appear within the broad absorption lines. It indicates either DN on the decline from outburst, or CV systems with low disk contribution where underlying stars provide most of the luminosity. Therefore, we do not provide the definite subtypes for these CV spectra. Finally, we classify 134 spectra in our sample as DN candidates.

Nova-like Variables (NL). Most of the spectral lines listed in Table 1, such as He I, appear in the spectra of NL. Besides, there are also some other emission lines, especially more and stronger high-excitation emission lines present in NL spectra, which are listed in Table 2. One critical characteristic is that He II $\lambda 4686$ and/or C III/N III $\lambda 4650$ are relatively stronger, and the former line may even be stronger than H β in the NL spectra. Moreover, a few additional spectral lines (as seen in Table 2) are also often detectable in the NL spectra, such as C II

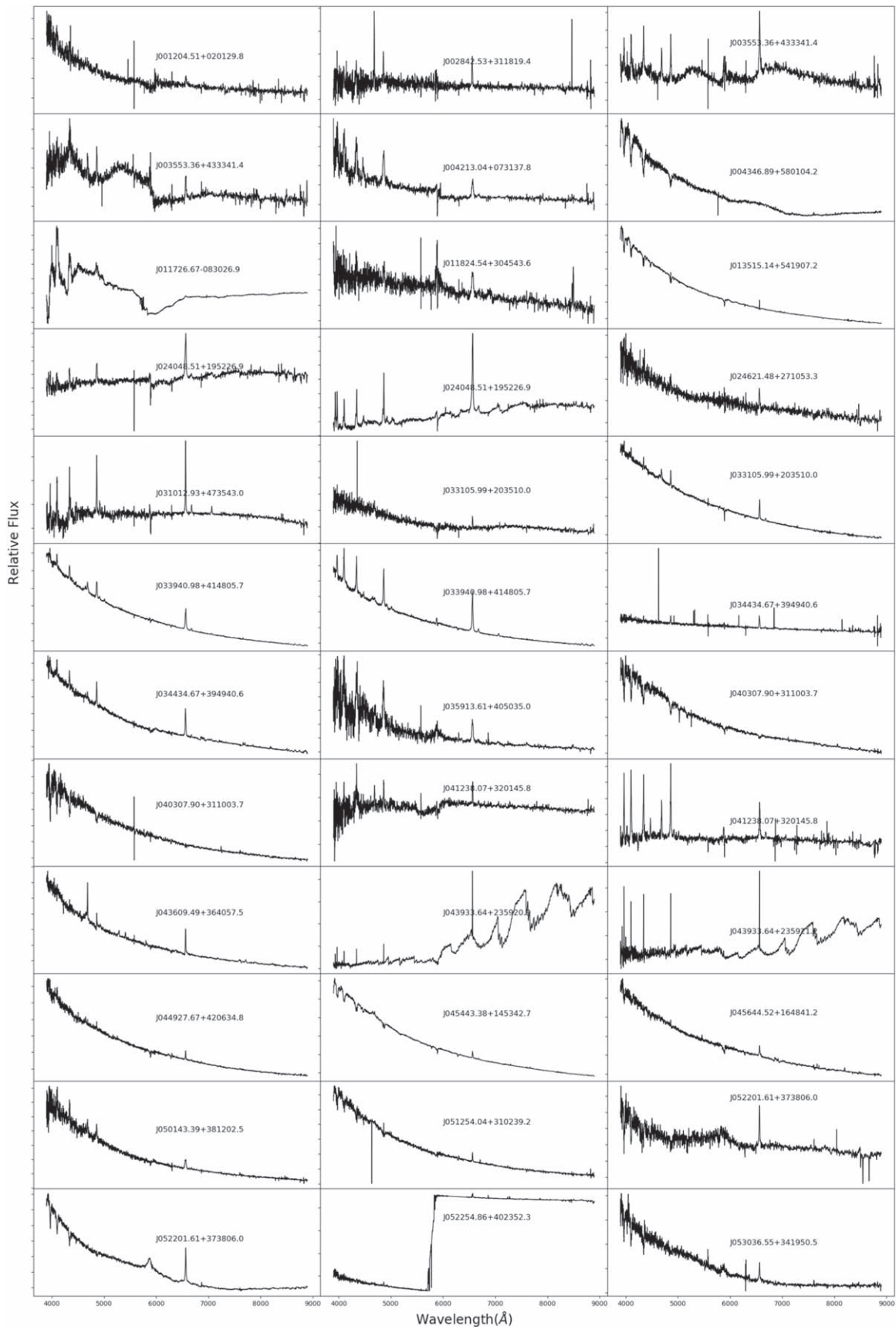


Figure 13. 71 spectra of the 58 new discoveries. The horizontal x-axis represents the wavelength coverage ranging from 3900 to 8900 Å, and the vertical y-axis represents the relative flux.

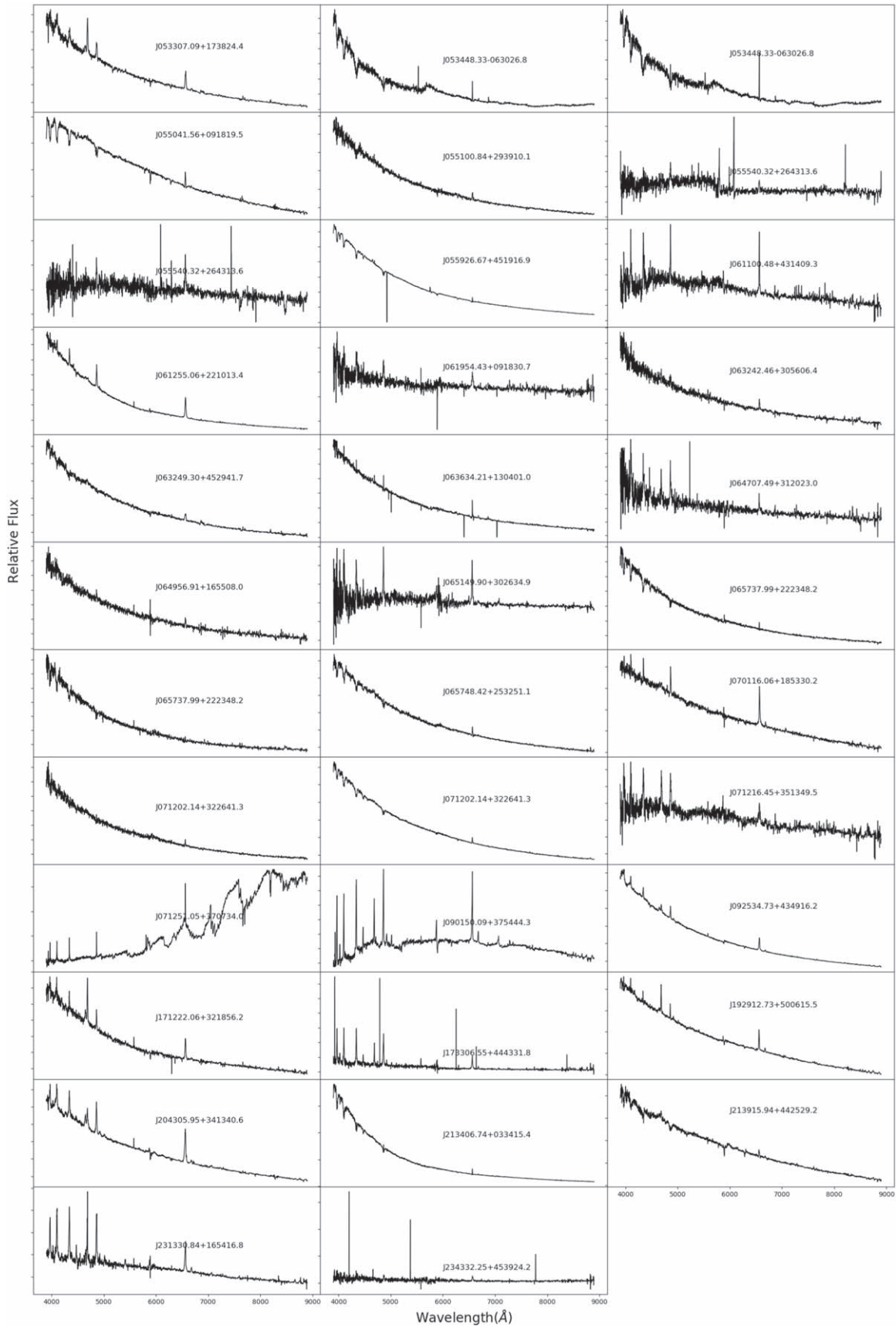


Figure 13. (Continued.)

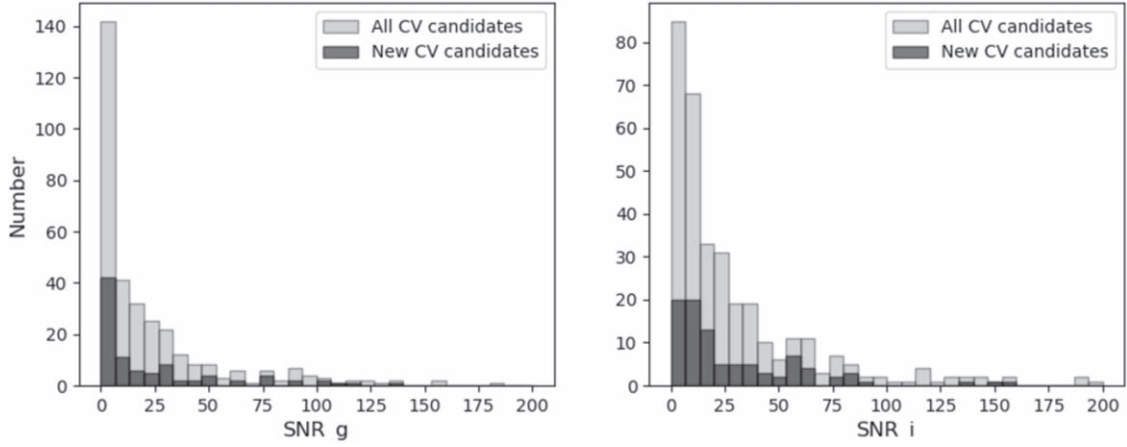


Figure 14. Distribution of S/N for CV candidates from LAMOST DR5. The left panel is the S/N distribution of the g band, and the right panel is S/N distribution of the i band. All of the candidates and new ones are respectively represented by gray and black.

$\lambda 4267$, $\lambda 7234$, and He II $\lambda 4542$. Similarly, we examine the ratio of He II $\lambda 4686$ to $H\beta$ for spectra that are marked as NL in the literature, and find that 14 out of 18 spectra of NL have values larger than 0.5. Therefore, CVs that have strong He II $\lambda 4686$, $H\beta$ emission lines, and the value of He II $\lambda 4686/H\beta > 0.5$ are considered candidates of NL. In addition, an obvious emission of C III/N III $\lambda 4650$ appearing in the spectra is also considered as a criterion of NL candidates. Meanwhile, we make a further identification by individually checking whether the spectra have the high-excitation emission lines such as C II $\lambda 4267$, $\lambda 7234$. As a result, 41 spectra in our sample are classified as NL candidates. Spectra of NL from LAMOST DR5 are shown in Figure 6. Apart from Balmer series, He II $\lambda 4686$ and C III/N III $\lambda 4650$ blend, we also mark some unique emission lines in the NL spectra by different colors.

Magnetic CVs. According to Warner (2003), magnetic CVs are usually included among NL, and the polars and the intermediate polars are two types of magnetic CVs. From the perspective of spectral classification, the spectra of this group of CVs are distinguished using the prominent characteristic lines of He I, He II, and C III/N III $\lambda 4650$ blend. Additionally, the strength ratio $H\beta/\text{He II } \lambda 4686$ could be used to distinguish polars and intermediate polars. For polars, these two lines are comparable, while for intermediate polars, He II $\lambda 4686$ is generally slightly weaker than $H\beta$ (Warner 2003). However, because the characteristics mentioned above resemble those of NL, we are not able to provide an accurate classification. Therefore, CVs that have the ratio of He II $\lambda 4686$ to $H\beta$ larger than 1 as well as strong He I, He II, and the C III/N III blend at 4650 \AA are considered as the candidates of magnetic CVs. Among the sample, 19 spectra are classified as the candidates of magnetic CVs. Two spectra of magnetic CV from LAMOST DR5 are shown in Figure 7. As seen in Figure 7, He II $\lambda 4686$ is extremely strong in both spectra, where intensity obviously exceeds that of $H\beta$ indicating a probable existence of a magnetic field.

High-inclination System. The systems with high inclination typically show very prominent central absorption in Balmer emission lines with the central depression sometimes reaching to the continuum level around the higher order lines. The 89 CVs in our sample showing obvious double-peaked emission lines are probably high-inclination systems. Examples of possible high-inclination systems are shown in Figure 8, in

which the Balmer line profiles for both spectra are also zoomed in.

Systems Showing the Secondary Stars. By inspecting 380 spectra of CVs, there are 33 systems that show spectral signatures from the secondary because of the appearance of the TiO band at 7100 \AA . This obvious feature reveals that each of them has an M-type secondary, probably indicating the existence of a tenuous disk with a low-mass transfer rate, or a pre-CV system without a mass transfer rate, of which the emission lines are generated by the secondary star. There is another explanation that the low disk luminosity may be due to the high-inclination effect, such as the system plotted in the bottom panel of Figure 9. For all the cases, the primary and secondary stars of the systems contribute most of the luminosity so that spectral features of the underlying stars can be observed. Figure 10 shows two spectra of CVs showing the M secondaries. In the spectrum of the top panel, the feature of the 7100 \AA band indicates the presence of an M-type star, and very narrow emission line cores appear in Balmer series which are likely generated by the M secondary. In the bottom panel, the CV spectrum exhibits not only the characteristics of a companion M star, but also double-peak features of spectral lines. Therefore, the CV probably has an edge-on disk that contributes a small portion of light.

4.2. Basic Distributions

To better understand the CV samples found in LAMOST DR5, we present some distributions of the sample. Figure 10 shows the spatial distributions of CVs from LAMOST, SDSS, Catalina, and the published catalogs. For CVs from the SDSS survey, the targets are distributed in the area of higher galactic latitude. For CVs from the Catalina survey, there is a gap existing in the galactic plane owing to its observation strategy. While for the sample selected from LAMOST DR5, the spatial distribution of CVs follows the footprint of the LAMOST survey, in which part of CVs are found at the low galactic latitude, especially in the direction of the Galactic Anticenter.

The magnitude distributions of the g and i bands for CVs from the published catalogs, Catalina, SDSS, and LAMOST surveys are shown in Figure 11. From the figure we can see that CVs from the spectroscopic surveys of SDSS and LAMOST are respectively distributed in the faint and bright ends. In

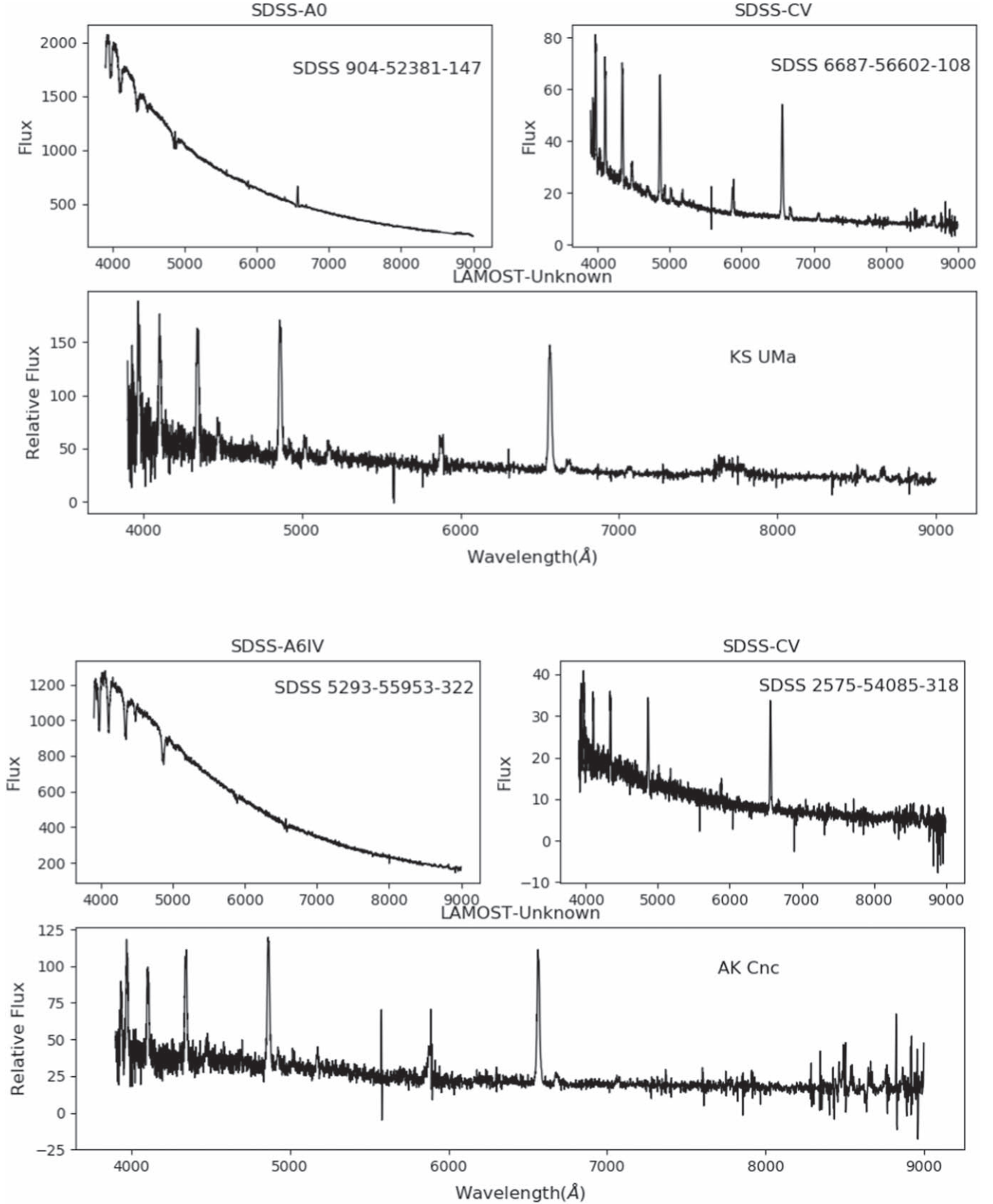


Figure 15. Spectra of two CVs from the LAMOST and SDSS surveys. For each CV, two spectra plotted in the top panels are from SDSS DR14, which are in the states of outburst and quiescence, respectively. The quiescent spectra from LAMOST DR5 are plotted in the bottom panels.

general, CVs from the LAMOST data are about 2 or 3 mag brighter than those from Catalina and SDSS.

We also use the astrometric and photometric data from *Gaia* to plot CVs in the CaMD. CVs found in this work, together

with those published in previous catalogs, are cross-matched with the *Gaia* data, their parallax, the mean G-band photometry, and the color of mean G_{BP} –mean G_{RP} are obtained. To compare the locus of CVs in CaMD with the main sequence

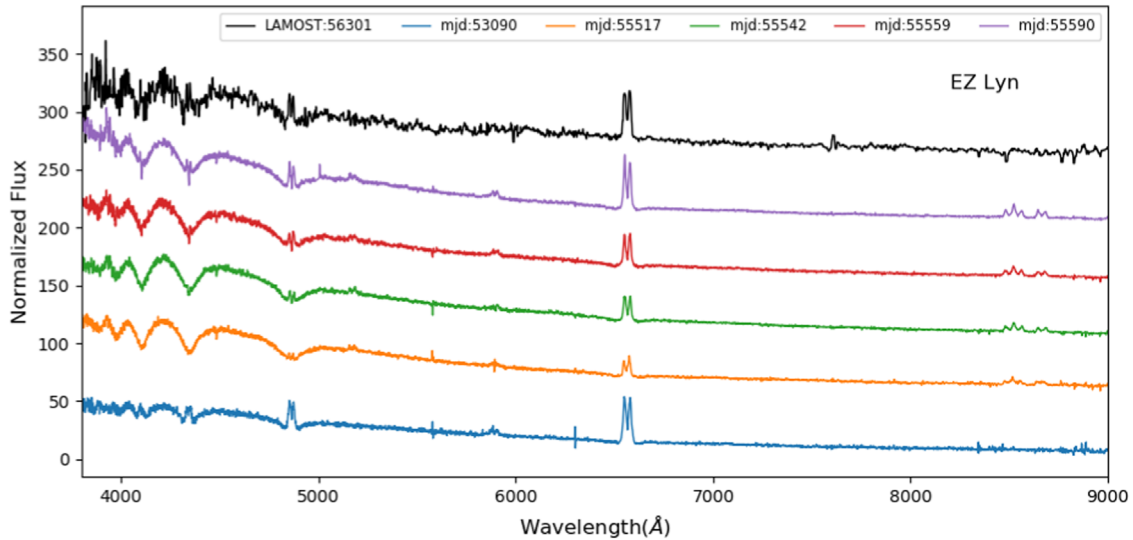


Figure 16. Spectra showing the outburst of LAMOST J080434.19+510349.4 (EZ Lyn). This series of spectra are plotted with time. The top spectrum is the latest one, which is observed by LAMOST. The bottom five spectra are picked up from SDSS survey.

and white dwarf sequence, a sample of 300,000 objects is selected from *Gaia* of which the parallaxes are greater than 10 mas and the relative parallax precisions are better than 20%. Figure 12 shows the *Gaia* CaMD, and we can see that the majority of CVs are located between the main sequence (the upper branch across diagonals) and the white dwarf sequence (the lower branch).

4.3. New Candidates

In the sample of CVs spectroscopically selected from LAMOST DR5, 71 spectra for 58 objects are new discoveries, which are shown in Figure 13. It should be noted that some artifacts may appear in the middle of the spectra, where the blue arms are combined with the red ones. The combination region in the LAMOST spectra is between 5700 and 5900 Å, which sometimes shows unreliable characteristics such as bumps due to the data procession. For example, a drop in the middle of spectrum of J011726.67–083026.9 and a steep rise in that of J052254.86+402352.3 are both caused by the processing method of combining the blue arms with the red arms. Another examples are J052201.61+373806.0, J053448.33–063026.8, and J053036.55+341950.5, which have broad emission lines in the combination region of the spectra. These characteristics are also very likely brought by the processing method, which must be cautiously dealt with when taking them into account. The distributions of S/N for CVs and new candidates selected from DR5 are shown in Figure 14. Among these objects, 31 spectra show blue continua and broad absorption Balmer lines, which are probably the DN undergoing outburst, NL similar to UX UMa, or any of the other systems with optically thick disks. Strong He II 4686 emission lines appear in the 31 spectra, in some of which the strength of He II are comparable to that of H β . Especially, there are eight spectra showing the likely polar nature that He II emission lines are much stronger than H β and the broad C III/N III 4650 Å blends are also present. Further identification needs more follow-up observations such as using the light curves to study their amplitudes and timescales of the variations. Besides, 12 spectra present absorption profiles with very narrow emission lines, among which there are eight

spectra also showing the feature of an M-type secondary. These new discoveries might belong to the group of pre-CVs.

4.4. Spectra of Common CVs in SDSS

We pick up spectra observed in different epochs from SDSS and LAMOST respectively for some CVs. Using a search radius of 5", we cross-match the sample of CV candidates from LAMOST DR5 with SDSS DR14 in order to check the spectra of same CVs from the SDSS data. Finally, a total of 143 spectra corresponding to 71 CVs are selected from SDSS DR14. Among those spectra, two CVs have spectra both during outburst and in quiescence, shown in Figure 15. For both CVs, the spectra plotted in the top left panels, which are classified as A-type stars by SDSS DR14, present broad absorption features of Balmer lines, as indicative of their stage of outburst. The spectra with strong emission lines plotted in the top right panels indicate that the CVs are at the stage of quiescence, of which the fluxes are almost decreased by one or two orders of magnitude. The amplitudes of the variabilities for the two CVs reveal that both of them are DNs.

In addition, we also obtain five observations of one CV in SDSS DR14 in Figure 16, which is undergoing burst. Four of these spectra are classified as hotter white dwarfs by the SDSS pipeline, and another one is classified as a CV. The spectrum from LAMOST is also plotted in black in Figure 16. From this group of spectra, we can see an obvious change in the emission line cores of Balmer series, especially in the lower order lines. Moreover, a deep absorption reversal in the emission components indicates that it is a possible high-inclination system.

4.5. Description of the Catalog

We provide a catalog of CVs selected from LAMOST DR5 that contains 12 columns. There are 380 spectra of CVs in the catalog, in which 71 spectra are newly discovered. The new discovered CV spectra are marked with an asterisk in the catalog. Table 3 lists 25 records in the catalog as examples, and the complete catalog can be downloaded.⁵ The first column of

⁵ http://paperdata.china-vo.org/Whou/CV/CVs_fitpath_DR5_info.csv

Table 3
The 25 Records of the Catalog Containing 12 Columns

| Designation | ID ^a | R.A. | Decl. | lmjd | Subtype LAMOST | Subtype Literature | C III/ N III | Fe II | Line Pro- file (H α) | H β / He4686 | He4686/H β |
|---------------------|-------------------------------|-------------|------------|-------|-------------------|-----------------------|-----------------|-------|---------------------------------|-----------------------|------------------|
| J003303.94+380105.4 | CRTS J003304.0+380105 | 8.2664481 | 38.018172 | 57313 | DN | CV | n | y | D | 9999 | 0 |
| J005347.32+405548.5 | SDSS J005347.32 +405548.5 | 13.447202 | 40.930155 | 57004 | MCV | CV | y | n | D | 0.55 | 1.82 |
| J013159.86+294922.0 | TT Tri | 22.99943 | 29.82278 | 56993 | DN | CV | n | y | S | 24.76 | 0.04 |
| J013737.21+300248.6 | TX Tri | 24.405066 | 30.046855 | 55918 | DN | DN | n | y | S | 8.18 | 0.12 |
| J020348.61+295925.6 | AI Tri | 30.95255 | 29.990469 | 56976 | MCV | Polar | y | n | S | 0.88 | 1.14 |
| J033352.81+332044.5 | PM J03338+3320 | 53.470042 | 33.345695 | 56633 | DN | CV | n | y | D | 9999 | 0 |
| J041329.22+311628.1 | 2MASS J04132921 +3116279 | 63.371783 | 31.274486 | 55949 | NL candidate | CV | y | n | S | 1.87 | 0.54 |
| J051922.90+155434.9 | CRTS J051922.9+155435 | 79.845419 | 15.909696 | 57313 | CV | CV | n | n | S | 27.14 | 0.04 |
| J052658.99+291508.3 | IPHAS J052659.00 +291508.4 | 81.745833 | 29.252333 | 55918 | NL candidate | CV | n | n | S | 1.6 | 0.62 |
| J052832.68+283837.6 | 1RXS J052832.5+283824 | 82.136208 | 28.643778 | 55910 | NL candidate | Polar | y | n | S | 1.78 | 0.56 |
| *J055540.32 | ... | 88.918024 | 26.720452 | 55899 | CV | None | n | n | S | 9999 | 0 |
| +264313.6 | | | | | | | | | | | |
| J064734.72+280622.1 | IR Gem | 101.89467 | 28.10615 | 55939 | DN | DN | n | y | S | 5.65 | 0.18 |
| *J064956.91 | ... | 102.48715 | 16.918906 | 57012 | CV | None | n | n | D | 9999 | 0 |
| +165508.0 | | | | | | | | | | | |
| *J065149.90 | ... | 102.95795 | 30.443034 | 55923 | CV | None | n | n | S | 9999 | 0 |
| +302634.9 | | | | | | | | | | | |
| J084427.11+125232.0 | AC Cnc | 131.1129683 | 12.8755573 | 56645 | CV | CV | n | n | D | 9999 | 0 |
| *J092534.73 | ... | 141.3947292 | 43.8211917 | 57419 | NL candidate | Star | y | n | S | 1.42 | 0.71 |
| +434916.2 | | | | | | | | | | | |
| J094431.73+035805.4 | VZ Sex | 146.132225 | 3.9681833 | 57821 | CV | DN | n | n | S | 9999 | 0 |
| J095148.96+340723.5 | RZ LMi | 147.9540125 | 34.1232083 | 56609 | CV | DN | n | n | S | −9999 | −9999 |
| J105430.43+300610.1 | SX LMi | 163.6268151 | 30.1028234 | 55907 | DN | DN | n | y | D | 9999 | 0 |
| J105656.99+494118.2 | CY UMa | 164.23749 | 49.688412 | 56411 | DN | DN | n | y | D | 9.11 | 0.11 |
| ‡J113122.39 | MR UMa | 172.8433 | 43.37738 | 57020 | DN | DN | n | y | S | 9999 | 0 |
| +432238.5 | | | | | | | | | | | |
| J125637.10+263643.2 | GO Com | 194.1546116 | 26.6120105 | 56396 | DN | DN | n | y | S | 9999 | 0 |
| J133941.12+484727.4 | V355 UMa | 204.92135 | 48.790961 | 56394 | DN | DN | n | y | D | 9999 | 0 |
| J161007.50+035232.7 | V519 Ser | 242.53129 | 3.8757684 | 56359 | CV | Polar | n | n | S | 9999 | 0 |
| *J173306.55 | ... | 263.2773 | 44.7255 | 57870 | NL candidates | None | y | n | S | 1.12 | 0.89 |
| +444331.8 | | | | | | | | | | | |

Note.

^a The previous identifications of known CVs.

(This table is available in its entirety in machine-readable form.)

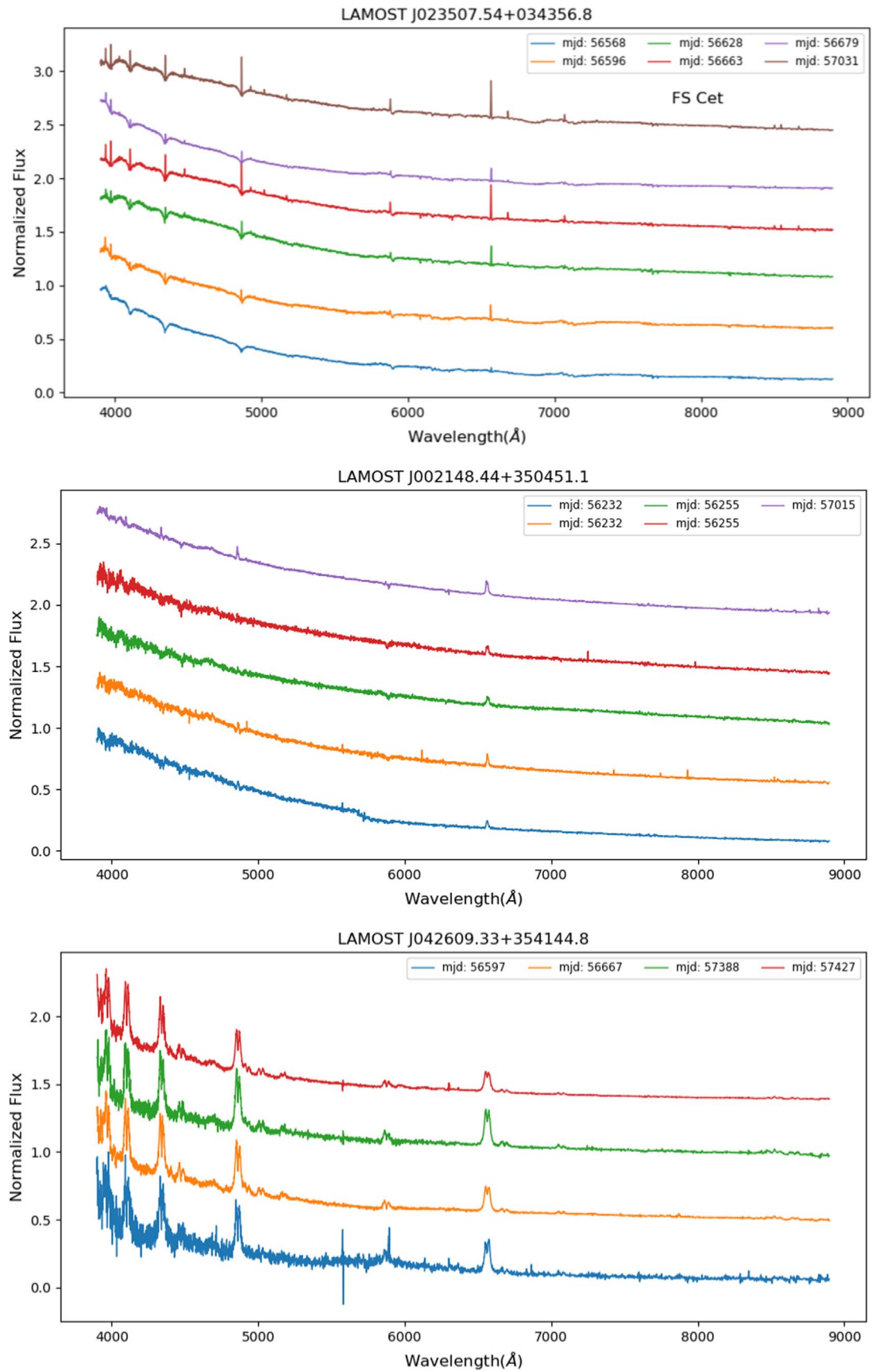


Figure 17. Examples of targets which have two, three, four, five, and six observations. In each panel, spectra are plotted by different colors, representing that they are observed at different epochs.

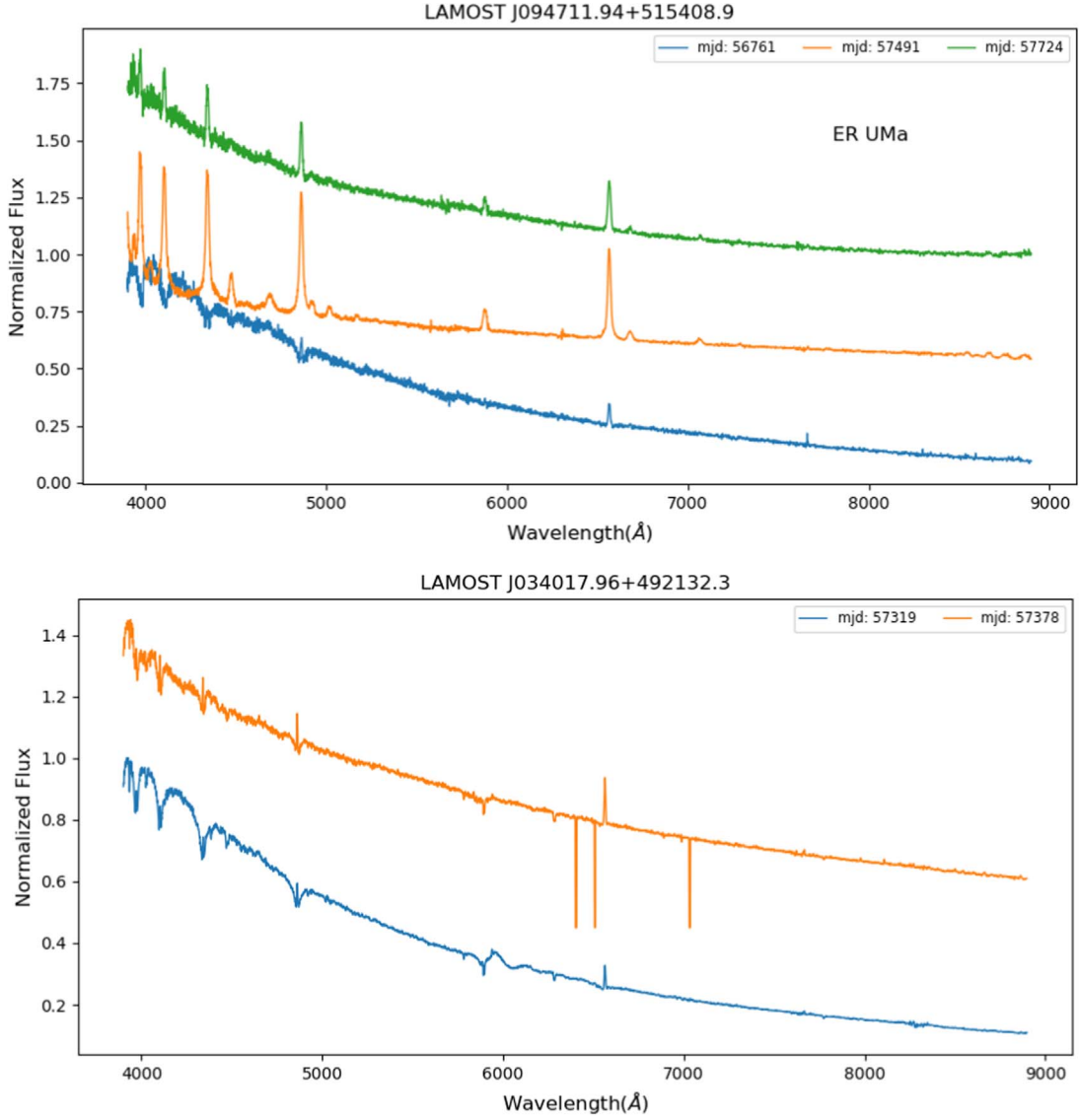


Figure 17. (Continued.)

the catalog gives the LAMOST designation for each target and the second column is the identifications of the objects in other literature if they have been previously identified as CVs. The third and fourth columns are the R.A. and Decl. of the targets, respectively. In order to distinguish multiple observations of the same source, we list the local modified Julian day (lmjd) of the observation date in the fifth column. The sixth column gives the subtypes of CVs, which are provided according to the spectral characteristics, including DN, NL, magnetic CV, or CV without exact classification whose counts are listed in Table 4. The seventh column of Table 3 displays the subtypes of CVs collected from the literature. Whether the spectra have C III/N III and Fe II emission lines are indicated in the eighth and ninth columns, respectively, while the shapes of the $H\alpha$ line profiles are marked as S or D for single-peak or double-peak in the tenth column. In the last two columns, two inverse ratios of line strength $H\beta/\text{He II } \lambda 4686$ and $\text{He II } \lambda 4686/H\beta$ are given because they are used as criteria for classifying DN and NL, respectively. It is noted that the values of these two ratios might be set to 0, 9999 or -9999 in some cases. The ratios of $H\beta/\text{He II } \lambda 4686$ and $\text{He II } \lambda 4686/H\beta$ are both assigned to

Table 4
Numbers of DN, NL, Magnetic CV, and the Remaining CVs without Exact Subtypes

| Subtype | DN | NL | Magnetic CV | CVs with No Subtypes |
|-------------------|-----|----|-------------|----------------------|
| Number of spectra | 134 | 41 | 19 | 186 |

Table 5
Frequency of Repeated Observations

| Observation frequency | 2 | 3 | 4 | 5 | 6 |
|-----------------------|----|----|---|---|---|
| Number of objects | 58 | 19 | 6 | 1 | 4 |

-9999 in the case where $H\beta$ lines appear in absorption and no He II $\lambda 4686$ emission lines are detected in the spectra. The two ratios are assigned to 0 and 9999 respectively in the case where $H\beta$ lines appear in absorption and He II $\lambda 4686$ emission lines are detected, and on the contrary they are assigned to 9999 and 0 in the case where $H\beta$ lines appear in emission and no He II $\lambda 4686$ emission lines are detected in the spectra. It also needs

to be noted that 23 spectra in our sample are observed in the test nights, which are not included in the released data. These 23 spectra are specially labeled with ‡ in the catalog.

5. Discussion and Summary

Using the rank-based algorithm in combination with the Random Forest algorithm, we pick out 380 spectra of 245 CVs from LAMOST DR5, among which 71 spectra of 58 CVs are new discoveries. According to the different spectral characteristics of subtypes, a part of the sample is given the subtypes including DN, NL, and magnetic CV. Besides, we also discuss the spectral features of the high-inclination systems and CVs showing the secondaries. We compare the spatial distributions, the magnitude distributions, and the *Gaia* CaMD locus for CVs from the LAMOST DR5, SDSS, and Catalina surveys. Through cross-matching, we find that some spectra of CVs are categorized as white dwarf or A-type stars in SDSS DR14. More interestingly, two targets that have both spectra in quiescence and during outburst in SDSS DR14, which should be classified as DN according to the variation of their luminosities. Besides, we also find that 88 CVs have been observed two or more times in the LAMOST survey. We count the frequencies of CVs having at least two spectra and list them in Table 5. The examples of objects which have repeated observations are shown in Figure 17. In particular, we note that the object having six observations in Figure 17 is well known as Feige 24 or FS Cet, which is a close binary system composed of a very hot white dwarf and an M-type main-sequence secondary (Holm 1976; Vennes et al. 2000). The spectral features of this system resemble those of CVs, while its Balmer emission lines are relatively narrower and generated from the partly ionized atmosphere of an M dwarf. From the spectra of some CVs with multiple observations, we can see that the dominated spectral features change from broad absorption lines to strong emission lines, which indicate that they are CVs in the states from the period of quiescence to outburst. In this paper, we mainly focus on the search of CVs in the LAMOST data set, the analysis of spectral characteristics of CVs, and the classification of CV subtypes. Further studies such as the analysis of orbital periods will be carried out using the time-domain medium-resolution spectra observed in the phase of LAMOST II, as well as follow-up photometric observations.

This work is supported by China Scholarship Council, the Joint Research Fund in Astronomy (grant no. U1931209) under

cooperative agreement between the National Natural Science Foundation of China and Chinese Academy of Sciences.

Guoshoujing Telescope (the Large Sky Area Multi-Object Fiber Spectroscopic Telescope, LAMOST) is a National Major Scientific Project built by the Chinese Academy of Sciences. Funding for the project has been provided by the National Development and Reform Commission. LAMOST is operated and managed by the National Astronomical Observatories, Chinese Academy of Sciences.

ORCID iDs

A-li Luo  <https://orcid.org/0000-0001-7865-2648>

References

- Breedt, E., Gänsicke, B. T., Drake, A. J., et al. 2014, *MNRAS*, **443**, 3174
- Coppejans, D. L., K rding, E. G., Knigge, C., et al. 2016, *MNRAS*, **456**, 4441
- Coppejans, D. L., Woudt, P. A., Warner, B., et al. 2014, *MNRAS*, **437**, 510
- Cui, X.-Q., Zhao, Y.-H., Chu, Y.-Q., et al. 2012, *RAA*, **12**, 1197
- Deng, L.-C., Newberg, H. J., Liu, C., et al. 2012, *RAA*, **12**, 735
- Downes, R., Webbink, R. F., & Shara, M. M. 1997, *PASP*, **109**, 345
- Downes, R. A., & Shara, M. M. 1993, *PASP*, **105**, 127
- Downes, R. A., Webbink, R. F., Shara, M. M., et al. 2001, *PASP*, **113**, 764
- Drake, A. J., G nsicke, B. T., Djorgovski, S. G., et al. 2014, *MNRAS*, **441**, 1186
- Du, C., Luo, A., Yang, H., Hou, W., & Guo, Y. 2016, *PASP*, **128**, 034502
- G nsicke, B. T., Dillan, M., Southworth, J., et al. 2009, *MNRAS*, **397**, 2170
- Han, X. L., Zhang, L.-Y., Shi, J.-R., et al. 2018, *RAA*, **18**, 068
- Holm, A. V. 1976, *ApJL*, **210**, L87
- Hou, W., Luo, A.-L., Hu, J.-Y., et al. 2016, *RAA*, **16**, 138
- Jiang, B., Luo, A., Zhao, Y., & Wei, P. 2013, *MNRAS*, **430**, 986
- Kogure, T., & Leung, K.-C. 2007, *ASSL*, **342**, 1
- Li, Y.-B., Luo, A.-L., Du, C.-D., et al. 2018, *ApJS*, **234**, 31
- Luo, A.-L., Zhang, H.-T., Zhao, Y.-H., et al. 2012, *RAA*, **12**, 1243
- Luo, A.-L., Zhao, Y.-H., Zhao, G., et al. 2015, *RAA*, **15**, 1095
- Mr z, P., Udalski, A., Poleski, R., et al. 2015, *AcA*, **65**, 313
- Szkody, P., Anderson, S. F., Ag eros, M., et al. 2002, *AJ*, **123**, 430
- Szkody, P., Anderson, S. F., Brooks, K., et al. 2011, *AJ*, **142**, 181
- Szkody, P., Anderson, S. F., Hayden, M., et al. 2009, *AJ*, **137**, 4011
- Szkody, P., Fraser, O., Silvestri, N., et al. 2003, *AJ*, **126**, 1499
- Szkody, P., Henden, A., Ag eros, M., et al. 2006, *AJ*, **131**, 973
- Szkody, P., Henden, A., Fraser, O., et al. 2004, *AJ*, **128**, 1882
- Szkody, P., Henden, A., Fraser, O. J., et al. 2005, *AJ*, **129**, 2386
- Szkody, P., Henden, A., Mannikko, L., et al. 2007, *AJ*, **134**, 185
- Vennes, S., Polonski, E. F., Lanz, T., et al. 2000, *ApJ*, **544**, 423
- Warner, B. 2003, *Cataclysmic Variable Stars* (Cambridge: Cambridge Univ. Press)
- Wenger, M., Ochsenein, F., Egret, D., et al. 2000, *A&AS*, **143**, 9
- Woudt, P. A., Warner, B., de Bude, D., et al. 2013, *MNRAS*, **421**, 2414
- Zhao, G., Zhao, Y.-H., Chu, Y.-Q., Jing, Y.-P., & Deng, L.-C. 2012, *RAA*, **12**, 723